Supporting Information

Exclusively Catalytic Hydrogenation of Nitrobenzene toward p-Aminophenol Over Atomically Precise $Au_{36}(SR)_{24}$ Clusters

Jinzhi Lu,[a] Kun Tang,[b] Guodong Qi,[c] Chao Juan,[d] Jun Xu,[c] Zhenfeng Cai,[d] Dan Li,*[,d] Xiao Cai,[a] Xu Liu,[a] Mingyang Chen,*[,b] Weiping Ding,[a] and Yan Zhu*[,a]

[a]Key Lab of Mesoscopic Chemistry of MOE and Jiangsu Key Lab of Vehicle Emissions Control, School of Chemistry and Chemical Engineering, Nanjing University, Nanjing 210093, China

[b]School of Materials Science and Engineering, University of Science and Technology Beijing, Beijing 100083, China

[c]State Key Laboratory of Magnetic Resonance and Atomic and Molecular Physics, Chinese Academy of Sciences, Wuhan 430071, China

[d]Key Laboratory of Green Chemistry and Technology of Ministry of Education, College of Chemistry, Sichuan University, Chengdu 610064, China

1. Experimental Section

Synthesis of $Au_{36}(DMBT)_{24}$: $Au_{36}(DMBT)_{24}$ cluster was synthesized using a two-step method.[S1] Step 1: 50 mg of $HAuCl_4 \cdot 3H_2O$ dissolved in 1 mL pure water was mixed with 10 mL CH_2Cl_2 containing tetraocty-lammonium bromide (TOAB; 80 mg). After vigorously stirring for 20 min, the organic layer was transferred into a 50 mL flask and 60 μL 3,5-dimethylbenzenethiol (DMBT) was injected. The above mixture was stirred until the color of the solution was clear, and then an aqueous solution containing 25 mg $NaBH_4$ was added. The reduction was allowed to proceed for 6 h. After that, the reaction mixture was dried by a rotary evaporator, and the obtained precipitates were washed

with methanol three times. Step 2: the obtained precursor was extracted with 0.5 mL toluene and then etched by 0.5 mL DMBT for 48 h at room temperature. The crude product was washed with CH_3OH and separated by thin-layer chromatography. $Au_{36}(DMBT)_{24}$ clusters were crystallized in toluene/acetonitrile solution by vapor diffusion over two weeks.

Synthesis of $Au_{36}(TBBT)_{24}$: $Au_{36}(TBBT)_{24}$ cluster was synthesized by a size focusing process.[S2] 100 mg $HAuCl_4 \cdot 3H_2O$ in 2 mL pure water was added to 15 mL CH_2Cl_2 solution containing TOAB (154 mg). After vigorously stirring for 30 min, the water phase was removed and then 125 μL TBBT (4-tert-butyl-benzenethiolate) was added to the organic phase. The solution was vigorously stirred in an ice bath for 3 h and then 3 mL aqueous solution containing 47 mg $NaBH_4$ was quickly added to the cold reaction mixture. The reduction was allowed to proceed overnight. The reaction product was evaporated and washed with methanol for three times. Poly-dispersed $Au_x(TBBT)_y$ was obtained. Subsequently 300 μL TBBT was added to the $Au_x(TBBT)_y$ precursor in 3 mL toluene under 80 °C for 2 h. The crude products dissolved in 5 mL dichloromethane (DCM) were separated on PTLC plate. The final solids were dissolved in CH_2Cl_2 and centrifugated at 10,000 rpm. The solvent was evaporated to give the $Au_{36}(TBBT)_{24}$.

Synthesis of $Au_{25}(SC_2H_4Ph)_{18}$: $Au_{25}(SC_2H_4Ph)_{18}$ clusters were prepared according to the previous method.[S3] 0.203 mmol $HAuCl_4 \cdot 3H_2O$ and 0.235 mmol TOAB were dissolved in 15 mL tetrahydrofuran in an ice bath. Until the above solution turned a wine red (30 min), 140 μL phenylethanethiol was added immediately the above solution. The mixture was slowly stirred about 1~3 h, and then 5 mL cold water of 78 mg $NaBH_4$

was quickly added. After stirring for 3 h, the ice water bath was removed. Then, the mixture solution was stirred to proceed overnight. The obtained product was washed with methanol five times. Finally, $Au_{25}(SC_2H_4Ph)_{18}$ clusters were extracted with CH_3CN.

Synthesis of $Au_{28}(TBBT)_{20}$: $Au_{28}(TBBT)_{20}$ clusters were synthesized by reacting $Au_{25}(SC_2H_4Ph)_{18}$ clusters with excess TBBT under 80 °C.[S4] 10 mg $Au_{25}(SC_2H_4Ph)_{18}$ was added to the mixture of 0.5 mL toluene and 0.5 mL TBBT. The reaction solution was heated at 80 °C for 2 h. The reaction product was washed with methanol three times. Finally, $Au_{28}(TBBT)_{20}$ clusters were extracted with CH_2Cl_2.

Synthesis of $Au_{44}(TBBT)_{28}$: $Au_{44}(TBBT)_{28}$ was prepared according to the synthesis of $Au_{36}(TBBT)_{24}$. The crude products dissolved in 5 mL DCM were separated on PTLC plate. A knife was used to cut the bands in the PTLC plate, and then the final solids were dissolved in CH_2Cl_2 and centrifugated. The solvent was evaporated to give the products $Au_{36}(TBBT)_{24}$ and $Au_{44}(TBBT)_{28}$, respectively.

Pt/C: The 5%Pt/C catalyst used in the work was purchased from Macklin without further purification.

Synthesis of ligand-off gold catalyst: The carbon black support was stirred in a solution of $Au_{36}(SR)_{24}$ in DCM at room temperature for 12 h. Then a rotary evaporator was used to remove the solvent at 30 °C. The sample was calcined at 250 °C in an Ar atmosphere for 2 h with a heating rate of 2.5 °C/min. Finally, it was cooled to room temperature in an Ar atmosphere to obtain the ligand-off gold catalyst.

Catalytic hydrogenation of nitrobenzene

Catalytic hydrogenation of nitrobenzene was performed in a 50 mL stainless-steel autoclave. Typically, 3 mg catalyst, 10 mg CTAB and 0.5 mmol nitrobenzene were added into sulfuric acid solution. First, the reactor was purged with N_2 several times to replace the air in the system, and the batch reactor was purged with H_2. The reaction system was heated to 120 °C with a continuous stirring rate of 1000 r/min, and kept at this temperature for 24 h. After the reaction, the reactor was cooled to room temperature naturally, and the catalyst was filtered. The cluster catalyst was washed with methanol, and dried at 60 °C after each cycle of reaction. The fresh clusters were supplemented to 3 mg per cycle. The products analyzed by HPLC (Agilent 1260) equipped with the UV detector (254 nm) and a C18 column. The eluent was methanol/water (70/30). The nitrobenzene conversion and product selectivity were calculated according to the following equation:

$$Conversion\ (mmol/g_{cat}) = \frac{moles\ of\ nitrobenzene\ input - moles\ of\ nitrobenzene\ output}{mass\ of\ catalyst}$$

$$Selectivity(\%) = \left(\frac{moles\ of\ specific\ product}{total\ moles\ of\ all\ product}\right) * 100$$

Characterizations

The UV-vis optical spectra were characterized by a SHIMADZU UV-1800 spectrometer. Transmission electron microscope (TEM) images were obtained on a JEM-2100F operated at a voltage of 200 kV. H_2-D_2 exchange reactions were performed in a quartz reactor. Typically, the sample (10 mg) was pretreated with high-purity Ar at 393 K for 1 h followed by cooling to 0 ℃. The sample was treated in pure H_2 gas flow for 0.5 h. Then, pulses of high-purity D_2 were injected into a H_2 stream and the temperature raised to 120 ℃. H_2 (m/z = 2), D_2 (m/z = 4), and HD (m/z = 3) were

analyzed by mass spectrometry.

FTIR spectra of the clusters with time at 120 ℃ were recorded by a Bruker Tensor 27 instrument equipped with a transmission accessory and a high-temperature/pressure reaction chamber, and spectra were recorded after 64 scans at a resolution of 4 cm^{-1}. KBr disk was scanned as a background spectrum under Ar flow, and the dichloromethane solution of clusters was respectively dropped on the disk and then evaporated by an infrared lamp. FTIR spectra were collected at certain time intervals when the temperature was kept at 120 °C.

In situ FTIR experiments of nitrobenzene adsorption were conducted on a Bruker Tensor 27 FT-IR spectrometer. Before measurement, the sample was heated in Ar at 100 °C for 2 h to remove impurities on the sample surface, and then cooled to 25 °C. After the background spectrum was recorded, the bubbling device of nitrobenzene was installed at the outlet of Ar flow (60 mL/min), and in situ FTIR spectra of the samples were obtained at some time in the stage of nitrobenzene adsorption. During the desorption stage, the nitrobenzene bubbling device was removed, then purged with Ar flow (60 mL/min) at 120 °C, and IR spectra of the samples were collected at specific times. Time-resolved in situ FTIR spectra of the nitrobenzene with H_2 over the catalysts were monitored using a temperature-controlled gas-solid cell which allowed for the use of Bruker Tensor 27 system. In the measurement, the sample was pressed into a 13 mm diameter disk and placed in a gas-solid cell, Ar was injected at 120 °C to remove excess gas and water, filled with 4 MPa H_2, and the reaction was performed at 120 °C.

All solution ^1H NMR experiments were conducted on a Bruker Avance-III 500

spectrometer with a 11.7 T magnetic field, corresponding to a ^{1}H frequency of 500 MHz. The spin-spin relaxation time (T_2) was measured using the CPMG (Carr-Purcell-Meiboom-Gill) pulse sequence. 150 μL of a phenylhydroxylamine solution saturated in benzene was added to a 1.5 mm outer diameter glass capillary tube along with 5.0 mg of either a Pt/C or Au cluster catalyst. The glass capillary tube was then flame-sealed. As a control, a phenylhydroxylamine solution without any added catalyst was also prepared. For NMR measurement, the sealed glass capillary tube was transferred to a 5 mm NMR tube containing 0.4 mL chloroform-d ($CDCl_3$) for the deuterium lock solution. The protons in positions neighboring and para to the phenylhydroxylamine exhibited the strongest NMR signals in the ^{1}H NMR spectra. Therefore, these protons were used as representatives to compare the T_2 relaxation times of the entire phenylhydroxylamine molecule both with and without the catalysts added. All measurements were conducted at atmospheric pressure and room temperature.

Raman spectra were collected on XploRA PLUS, HORIBA Scientific, France, with a laser wavelength of 532 nm and intensity of 100 %. Reaction conditions: 120 °C, 40 mL of 0.5 mol/L sulfuric acid solution, 3 mg catalyst, 40 mg CTAB, 400 μL nitrobenzene, 2.0 MPa H_2, rotation speed 900 r/min.

Computational Methods

The reaction pathways for the hydrogenation and acid-aided dehydration reactions of $PhNO_2$ with and without the Au cluster catalysts were predicted. The $Au_{28}(SR)_{28}$, $Au_{44}(SR)_{28}$, and $Au_{36}(SR)_{24}$ cluster catalysts were modelled using the simplified $Au_n(SR)_m$ models with R = CH_3, built based on the crystal structures. To predict the

interconversion of the three clusters, presumably driven by the Au aggregation, the chemical potential of the solid gold is estimated at the same level of theory. In order to do so, pure Au_n clusters (n = 13, 19, 43, 55, and 79) were built using the Wulff construction on the fcc crystal structure and optimized at the DFT level; extrapolation of the chemical potentials for these clusters to $n \rightarrow \infty$ limit yield the approximate chemical potential for the fcc gold (solid). All of the calculations were performed at the density functional theory (DFT) level using Gaussian09 software suit.[S5] The Perdew–Burke–Ernzerhof[S6] (PBE) exchange-correlation functional and a LANL2DZ basis set and pseudopotential[S7,S8] were adopted for the DFT calculations.

2. Supporting Figures and Tables

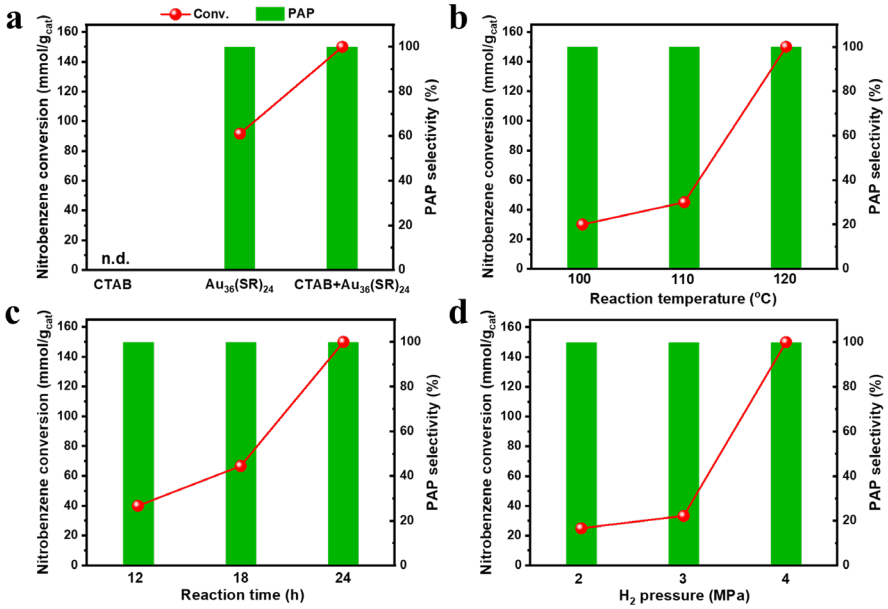

Fig. S1 Effects of reaction conditions on catalytic performances of $Au_{36}(SR)_{24}$ catalysts for nitrobenzene hydrogenation: (a) CTAB; (b) reaction temperature; (c) reaction time; (d) H_2 pressure. All the data were the average of the three reactions.

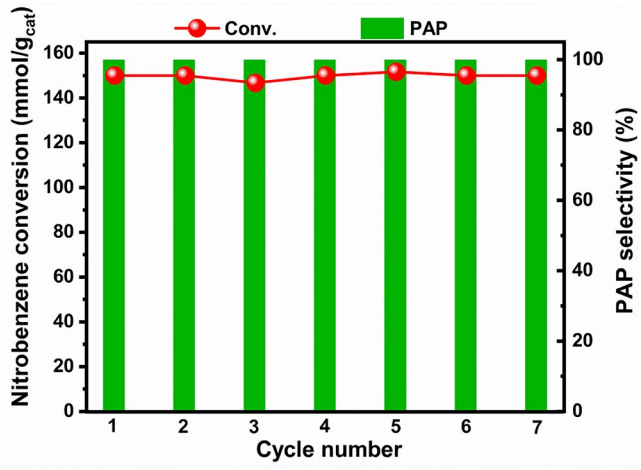

Fig. S2 Recyclability of $Au_{36}(SR)_{24}$ catalysts. Reaction conditions: 3 mg catalyst, 0.5 mmol nitrobenzene, 10 mg CTAB, 4 MPa H_2, 0.5 mol/L sulfuric acid solution, 120 ℃ for 24 h.

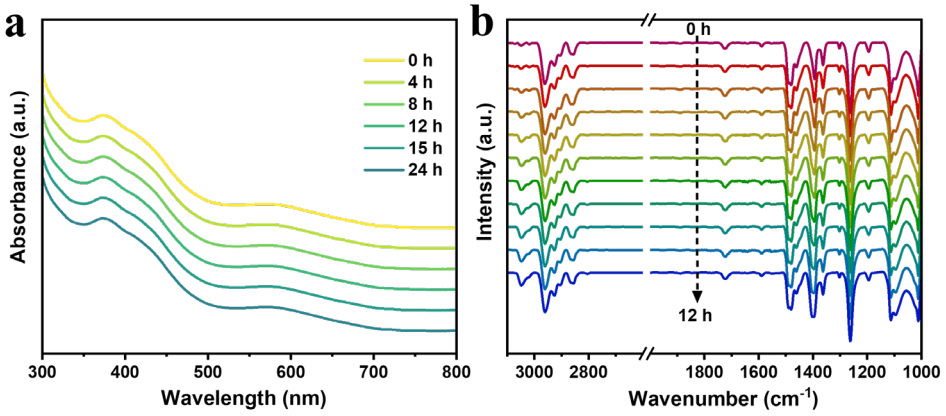

Fig. S3 (a) UV-vis spectra of $Au_{36}(SR)_{24}$ clusters at 120 ℃ in sulfuric acid solution (0.5 mol/L). (b) In situ FTIR spectra of $Au_{36}(SR)_{24}$ clusters at 120 ℃ in the Ar gas. UV-vis spectra of the $Au_{36}(SR)_{24}$ clusters under 120 ℃ in sulfuric acid solution (0.5 mol/L) were detected to determine the structural robust of the clusters under reaction conditions. In situ FT-IR spectra showed that the ligand of clusters had no obvious change during the reaction, further indicating that the $Au_{36}(SR)_{24}$ clusters were robust under reaction conditions.

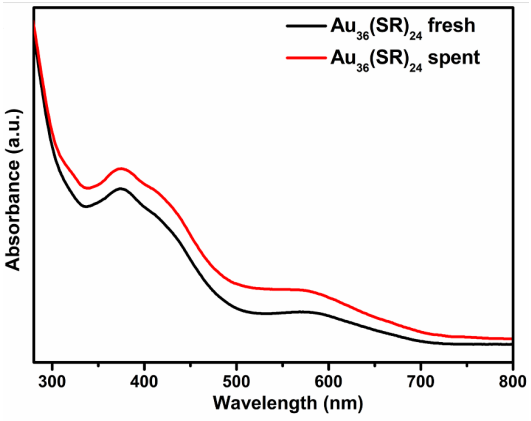

Fig. S4 UV-vis spectra of fresh and spent $Au_{36}(SR)_{24}$ clusters.

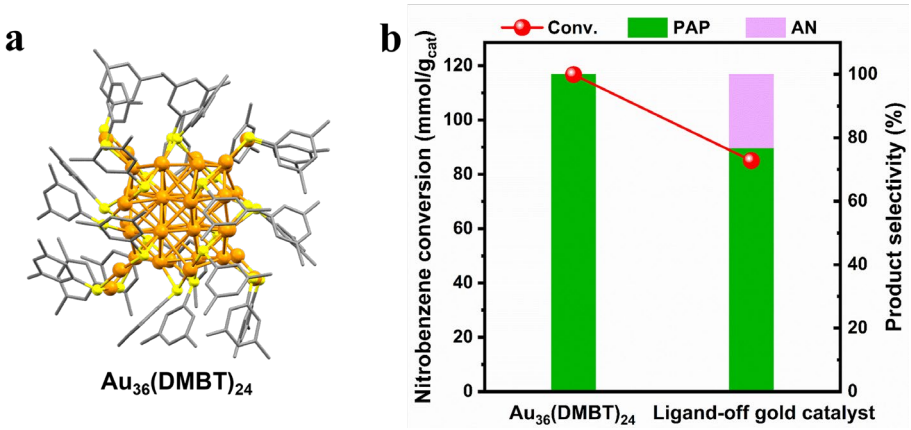

Fig. S5 (a) Crystal structure of $Au_{36}(DMBT)_{24}$. Color code: orange = Au; yellow = S; gray = C. The H atoms are omitted for clarity. (b) Catalytic performances of $Au_{36}(DMBT)_{24}$ and the ligand-off gold catalyst for the nitrobenzene hydrogenation.

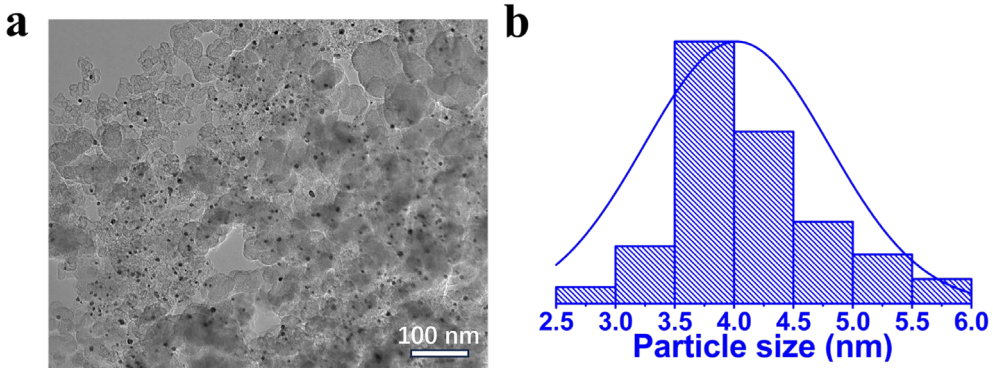

Fig. S6 (a) TEM image of the ligand-off gold catalyst. (b) The corresponding size distribution.

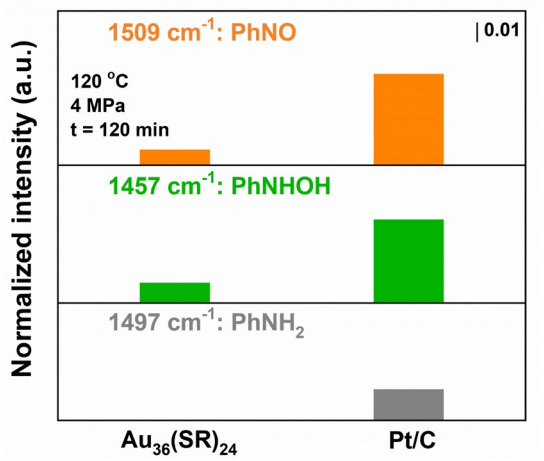

Fig. S7 The concentration for PhNO, PhNHOH and $PhNH_2$ over the $Au_{36}(SR)_{24}$ and Pt/C catalysts at 120 min of reaction from Figure 2c and d. The concentration of the species was semiquantitative from the band intensity.

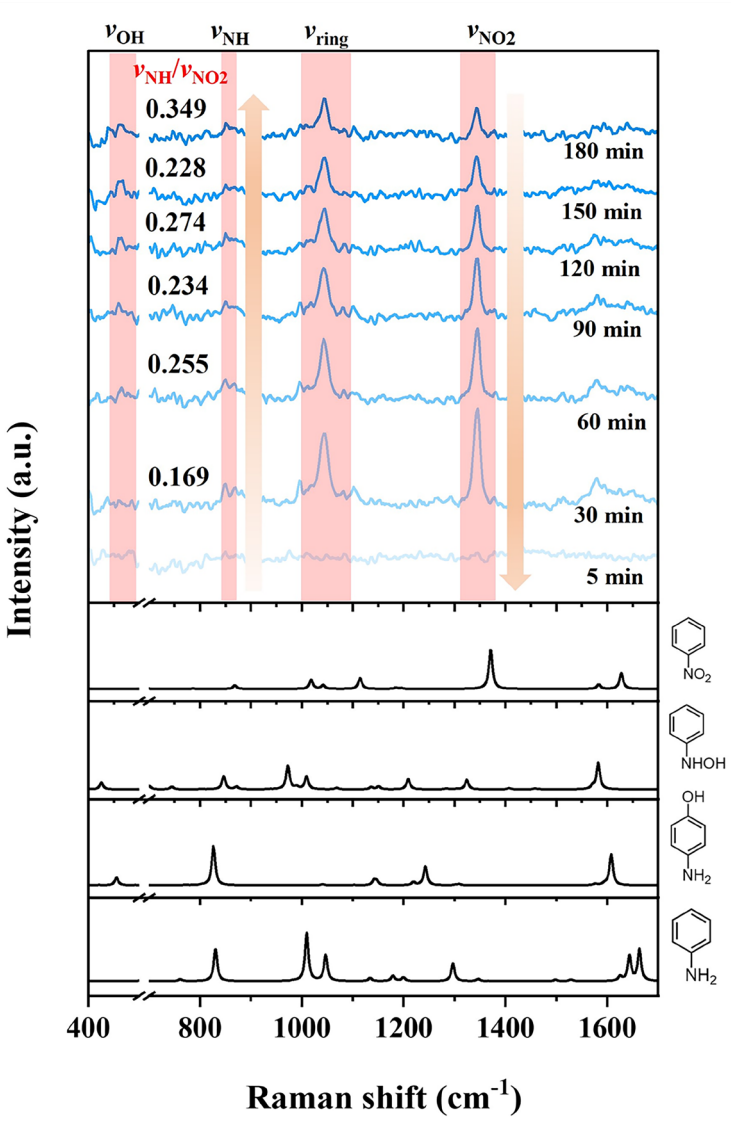

Fig. S8 In situ Raman spectra showing the reduction process of catalytic hydrogenation of nitrobenzene over $Au_{36}(SR)_{24}$ cluster. Calculated Raman spectra of nitrobenzene, PHA, PAP and aniline were plotted for comparison. (Reaction conditions: 120 ℃, 0.5 mol/L sulfuric acid solution, 3 mg catalyst, 40 mg CTAB, 400 μL nitrobenzene, 2.0 MPa H_2, rotation speed 900 r/min).

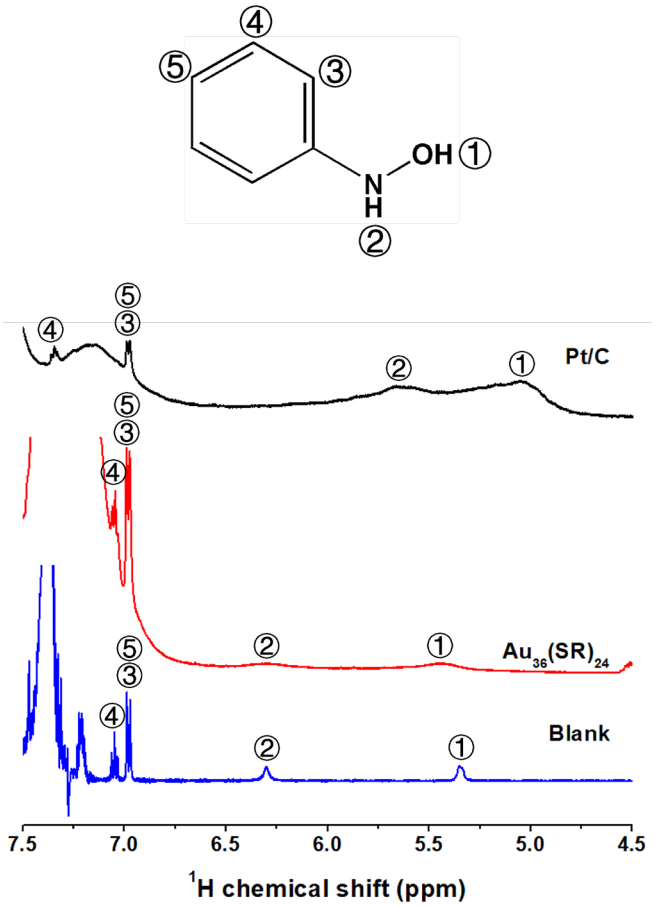

Fig. S9 ^{1}H NMR spectra obtained from PHA dissolved in benzene with or without addition of the catalysts.

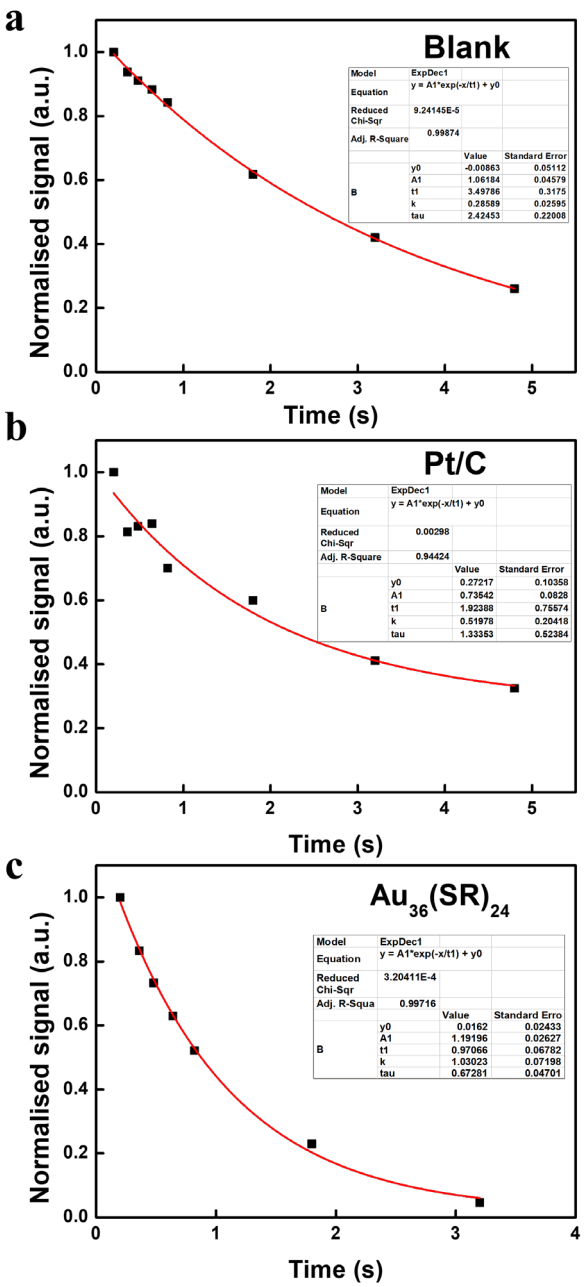

Fig. S10 T_2 CPMG relaxation data of PHA dissolved in benzene with or without catalysts: (a) Blank; (b) Pt/C catalyst; (c) $Au_{36}(SR)_{24}$. The fitting was based on the equation: $M_{xy}(2n\tau) = M_0 \exp(-2n\tau /T_2)$.

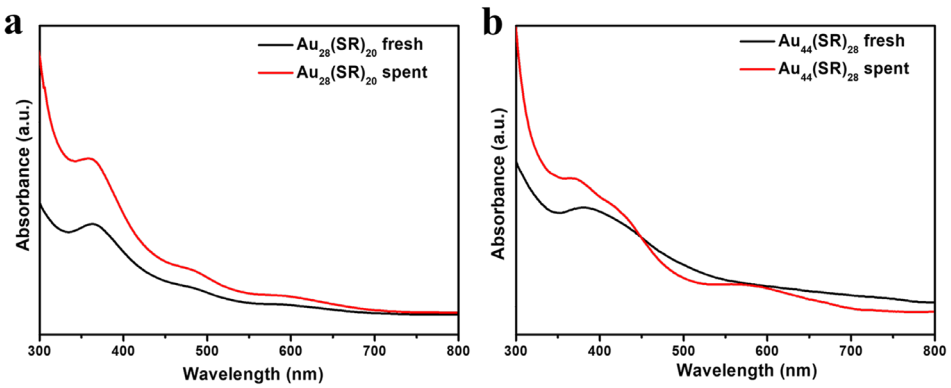

Fig. S11 (a) UV-vis spectra of fresh and spent $Au_{28}(SR)_{20}$ clusters. (b) UV-vis spectra of fresh and spent $Au_{44}(SR)_{28}$ clusters.

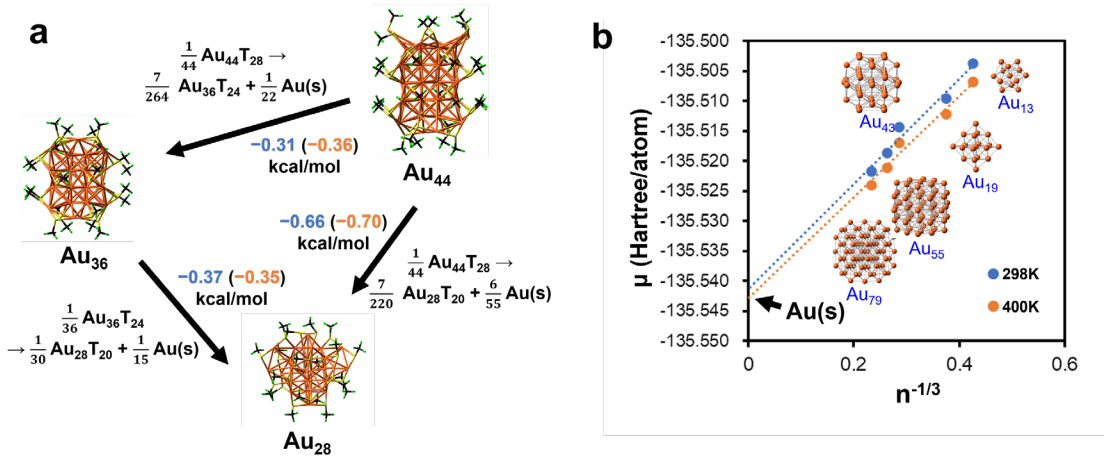

Fig. S12 Interconversion of $Au_{28}(SR)_{20}$, $Au_{36}(SR)_{24}$ and $Au_{44}(SR)_{28}$ clusters with solid Au formation. (a) The reaction energy per Au equivalence for the interconversion reactions at 298 K (blue) and 400 K (orange in parenthesis). (b) The fitting of solid Au energy (for the evaluation of interconversion reaction energies) using the method of least squares. The thermal stabilities of the three cluster catalysts are compared by examining the interconversion reactions. Considering the interconversion with solid Au yielded as aggregation product, the three clusters exhibit comparable stabilities in the order: $Au_{44}(SR)_{28}$ < $Au_{36}(SR)_{24}$ < $Au_{28}(SR)_{20}$. The conversion of the least stable $Au_{44}(SR)_{28}$ into $Au_{28}(SR)_{20}$ is exergonic by less than 1 kcal/mol per Au, implying the degradation of $Au_{36}(SR)_{24}$ and $Au_{28}(SR)_{20}$ requires non-ambient conditions. It is also found that raising the temperature increases the relative stability of $Au_{36}(SR)_{24}$ with respect to $Au_{28}(SR)_{20}$, while decreasing the relative stability of $Au_{44}(SR)_{28}$. Such prediction is consistent with the experimental founding that $Au_{44}(SR)_{28}$ partially turns into $Au_{36}(SR)_{24}$ during the highly exergonic reaction at 120 °C.

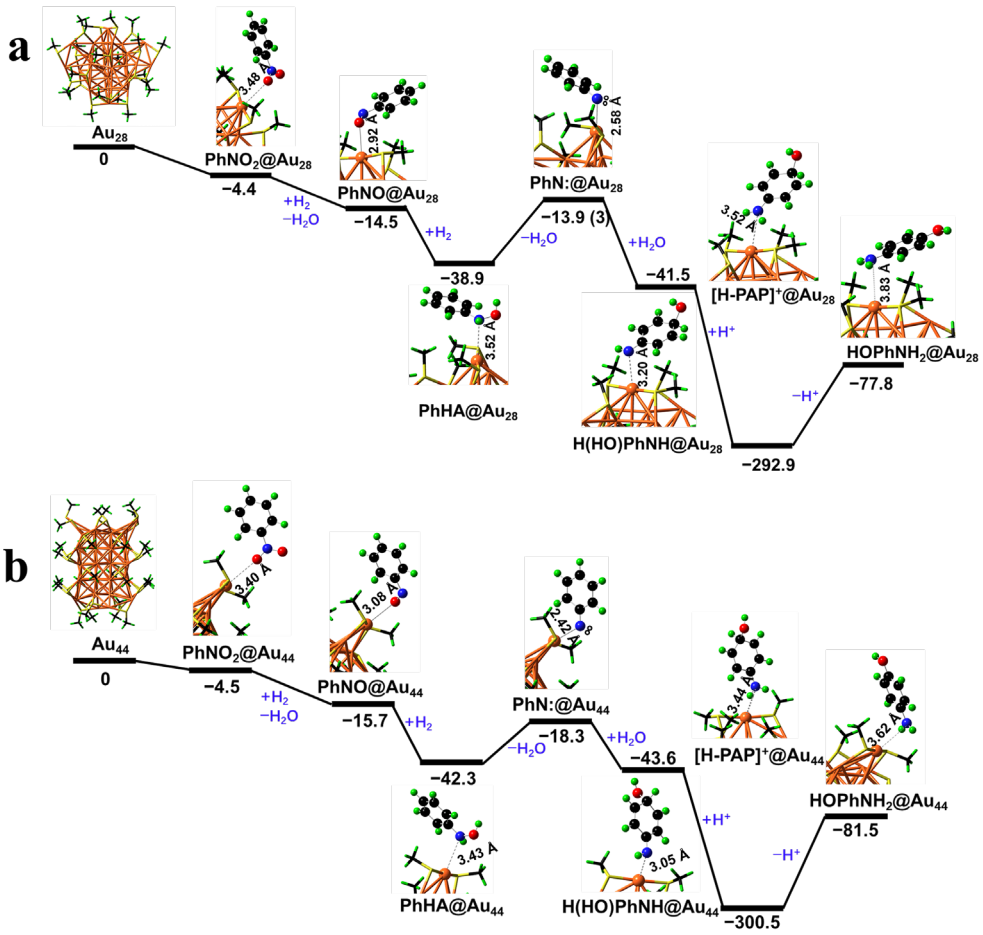

Fig. S13 The proton-transfer pathway with catalysts: (a) $Au_{28}(SR)_{20}$ cluster; (b) $Au_{44}(SR)_{28}$ cluster. The Gibbs free energies at 298 K are given in kcal/mol, the spin multiplicities are given in the parenthesis (singlet if omitted). The atomic color code: O = red, N = blue, C = black, H = green, Au = orange, and S = yellow. The unpaired electrons are indicated by the white circles. The distance between the active Au site and the organic species are labelled with texts.

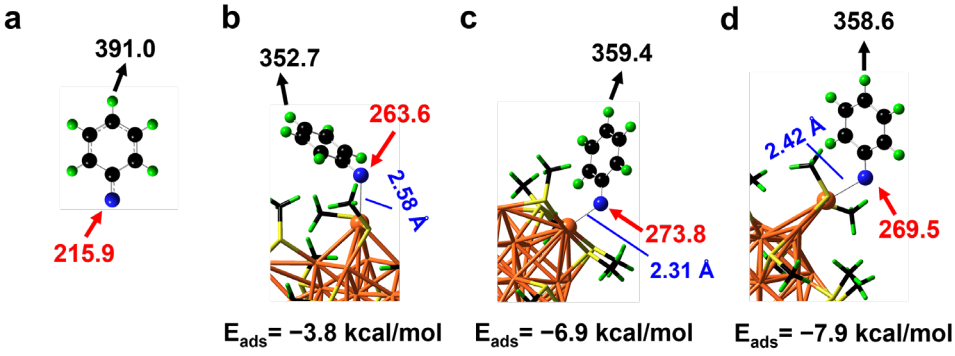

Fig. S14 Gas-phase deprotonation energy (DPE, black) for the para-H and proton affinity (PA, red) for N of PhN: (triplet) on (a) no catalyst, (b) $Au_{28}(SR)_{20}$, (c) $Au_{36}(SR)_{24}$, and (d) $Au_{44}(SR)_{28}$ at 298 K at the DFT level, respectively. The Gibbs free energies at 298 K are given in kcal/mol.

Table S1. Comparison of the activity and PAP selectivity for the nitrobenzene hydrogenation on the reported catalysts and this work's catalysts.

Catalyst	Acid	n(acid)/ n(nitrobenzene)	Nitrobenzene conversion (%)	PAP selectivity (%)	Reference
5 % Pd/C	H_3PO_4	2	90	61.1	S9
3%Pt/C-3	H_2SO_4	32.77	100	75	S10
Pt/C	H_2SO_4	0.5	99	81	S11
1.5% Pt/C	H_2SO_4	0.8	100	84.3	S12
1% Pt/5P-ACC	H_2SO_4	3.1	100	89.9	S13
Pt-Rh/AC	H_2SO_4	2.76	82.5	95.4	S14
1% Au/TiO_2	H_2SO_4	0.41	78	81	S15
3% Pt/C-2	H_2SO_4	1.26	97	74	S16
1% Pt/ZrP	H_2SO_4	1.15	96	89	S17
Ni/CN	H_2SO_4	65.07	43	100	S18
3 % Pt/C	H_2SO_4	0.55	100	88	S19
CNMC-2	H_2SO_4	66.5	47.5	99	S20
2%Pt/CMK-1	H_2SO_4	1.7	67	84	S21
Pt-S(thiourea)/C	H_2SO_4	1.29	99.8	72.5	S22
Pt/CS_3	H_2SO_4	1.28	98.4	65.1	S23
Pd@SOC	H_2SO_4	9.24	100	87.5	S24
$Au_{36}(SR)_{24}$	H_2SO_4	3	90	~100	This work
$Au_{44}(SR)_{28}$	H_2SO_4	3	62	~100	This work
$Au_{28}(SR)_{20}$	H_2SO_4	3	30	~100	This work

Supporting References

S1. X. Liu, W. W. Xu, X. Huang, E. Wang, X. Cai, Y. Zhao, J. Li, M. Xiao, C. Zhang, Y. Gao, W. Ding and Y. Zhu, *Nat. Commun.*, 2020, **11**, 3349.

S2. C. Zeng, Y. Chen, K. Iida, K. Nobusada, K. Kirschbaum, K. J. Lambright and R. Jin, *J. Am. Chem. Soc.*, 2016, **138**, 3950-3953.

S3. Z. Wu, J. Suhan and R. Jin, *J. Mater. Chem.*, 2009, **19**, 622-626.

S4. C. Zeng, T. Li, A. Das, N. L. Rosi and R. Jin, *J. Am. Chem. Soc.*, 2013, **135**, 10011-10013.

S5. M. J. Frisch, G. W. Trucks, H. B. Schlegel, G. E. Scuseria, M. A. Robb, J. R. Cheeseman, G. Scalmani, V. Barone, B. Mennucci, G. A. Petersson H. Nakatsuji, M. Caricato, X. Li, H. P. Hratchian, A. F. Izmaylov, J. Bloino, G. Zheng, J. L. Sonnenberg, M. Hada M. Ehara, K. Toyota, R. Fukuda, J. Hasegawa, M. Ishida, T. Nakajima, Y. Honda, O. Kitao, H. Nakai, T. Vreven, J. J. A. Montgomery, J. E. Peralta, F. Ogliaro, M. Bearpark, J. J. Heyd, E. Brothers, K. N. Kudin, V. N. Staroverov, R. Kobayashi, J. Normand, K. Raghavachari, A. Rendell, J. C. Burant, S. S. Iyengar, J. Tomasi, M. Cossi, N. Rega, N. J. Millam, M. Klene, J. E. Knox, J. B. Cross, V. Bakken, C. Adamo, J. Jaramillo, R. Gomperts, R. E. Stratmann, O. Yazyev, A. J. Austin, R. Cammi, C. Pomelli, J. W. Ochterski, R. L. Martin, K. Morokuma, V. G. Zakrzewski, G. A. Voth, P. Salvador, J. J. Dannenberg, S. Dapprich, A. D. Daniels, Ö. Farkas, J. B. Foresman, J. V. Ortiz, J. Cioslowski and D. J. Fox, Gaussian 09, Revision B.1, Gaussian, Inc., Wallingford CT, 2009.

S6. J. P. Perdew, K. Burke and M. Ernzerhof, *Phys. Rev. Lett.*, 1966, **77**, 3865-3868.

S7. T. H. Dunning and P. J. Hay, in *Modern Theoretical Chemistry*, Ed. H. F. Schaefer Ⅲ, Vol. 3: Plenum, New York, 1977, 1-28.

S8. J. P. Hay and W. R. Wadt, *J. Chem. Phys.*, 1985, **82**, 299-310.

S9. A. Zoran, O. Khodzhaev and Y. Sasson, *J. Chem. Soc. Chem. Commun.*, 1994, **19**, 2239-2240.

S10. C. V. Rode, M. J. Vaidya and R. V. Chaudhari, *Org. Process Res. Dev.*, 1999, **3**, 465-470.

S11. R. Joncour, A. Ferreira, N. Duguet and M. Lemaire, *Org. Process Res. Dev.*, 2018, **22**, 312-320.

S12. S. K. Tanielyan, J. J. Nair, N. Marin, G. Alvez, R. J. McNair, D. Wang and R. L. Augustine, *Org. Process Res. Dev.*, 2007, **11**, 681-688.

S13. Y. Liu, Y. Sheng, Y. Yin, J. Ren, X. Lin, X. Zou, X. Wang and X. Lu, *Acs Omega*, 2022, **7**, 11217 11225.

S14. Y. Sheng, Y. Liu, Y. Yin, X. Zou, J. Ren, B. Wu, X. Wang and X. Lu, *Chem. Eng. J.*, 2023, **452**, 139448.

S15. L. Zou, Y. Cui and W. Dai, *Chinese J. Chem.*, 2014, **32**, 257-262.

S16. J. M. Nadgeri, N. S. Biradar, P. B. Patil, S. T. Jadkar, A. C. Garade and C. V. Rode, *Ind. Eng. Chem. Res.*, 2011, **50**, 5478-5484.

S17. F. Zhang, Y. Jiang, S. Dai, X. Wei, Y. Ma, H. Liao, Y. Qin, Q. Peng, X. Zhao and Z. Hou, *Ind. Eng. Chem. Res.*, 2023, **62**, 5814-5825.

S18. T. Wang, Z. Dong, T. Fu, Y. Zhao, T. Wang, Y. Wang, Y. Chen, B. Han and W. Ding, *Chem. Commun.*, 2015, **51**, 17712-17715.

S19. C. V. Rode, M. J. Vaidya, R. Jaganathan and R. V. Chaudhari, *Chem. Eng. Sci.*, 2001, **56**, 1299-1304.

S20. T. Wang, Z. Dong, W. Cai, Y. Wang, T. Fu, B. Zhao, L. Peng, W. Ding and Y. Chen, *Chem. Commun.*, 2016, **52**, 10672-10675.

S21. K. I. Min, J. S. Choi, Y. M. Chung, W. S. Ahn, R. Ryoo and P. K. Lim, *Appl. Catal. A-Gen.*, 2008, **337**, 97-104.

S22. J. Luo, C. Yao, D. Ma, Y. Chen, M. Tian, H. Xie, R. Chen, J. Wu, Y. Zhen, L. Pan, C. Lu, F. Feng, X. Xu, Q. Wang, Q. Zhang and X. Li, *Appl. Catal. A-Gen.*, 2023, **660**, 119198.

S23. J. Luo, C. Zhang, C. Yao, D. Ma, Y. Chen, M. Tian, H. Xie, L. Pan, Y. Zhen, R. Chen, J. Wu, C. Lu, F. Feng, X. Xu, Q. Wang, Q. Zhang and X. Li, *Mol. Catal.*, 2023, **545**, 113216.

S24. C. Yin, Z. Xiang, Y. Yao, X. Li, C. Ma, X. Liu, Y. Zhou, W. He, C. Zhou, F. Feng, Q. Zhang, J. Lyu, Y. Liu, C. Lu and X. Li, *ACS Catal.*, 2023, **13**, 13756-13767.